2018 European Control Conference (ECC)
June 12-15, 2018. Limassol, Cyprus

The Impact of Deep Brain Stimulation on a Simulated Neuron: Inhibition, Excitation, and Partial Recovery

Helena Andersson[1], Alexander Medvedev[1], Ruben Cubo[1]

Abstract— **Deep Brain Stimulation (DBS) is an established therapy to alleviate the symptoms of neurological disorders such as Parkinson's Disease and Essential Tremor. Depending on the disease, a certain area of the brain is subjected to electrical stimuli through a surgically implanted lead. Despite the clinically proven effectiveness of DBS, the underlying biological mechanism is poorly understood. Two dominating theories seek to explain how the DBS therapy exerts effect on neurons, one through inhibition and another through excitation. This simulation study aims at demonstrating that both scenarios are feasible within the brain domain exposed to pulsatile electrical stimulation and conditional on the temporal relationship between the neural input and the DBS pulse sequence. Since some neurons in the targeted population are assisted to fire in response to the cumulative dynamical action of a stimulation pulse and neural input from a neighbouring neuron, a partial function recovery of the neural network is expected. Simulations with a spatially distributed deterministic neuron model support the presented hypothesis and provide insights into the role of DBS frequency and pulse width (duty cycle) in restoring the neural processing ability. The obtained results highlight the role of the phase difference between the neural input and the DBS pulse sequence in the neuron's response to stimulation.**

I. Introduction

Skeletal muscle is controlled by the Central Neural System (CNS) that consists of the brain and the spinal cord [1], [2]. CNS dynamically commands and coordinates muscle contractions that actuate the movement of body parts. The neuron is a basic unit of CNS. It receives input from other neurons through dendrites and produces output through the axon. Neural communication is an electric process, implemented through synaptic transmission and mediated by chemical messengers called neurotransmitters. Neurotransmitters are released from the axon terminal and bind to receptor sites on the post-synaptic cells [3].

A. Parkinson's disease and Essential tremor

Although the exact mechanisms behind neurological conditions such as Parkinson's disease (PD) and Essential tremor (ET) remain unknown, depletion of neurotransmitters, dopamine in PD and norepinephrine in ET, is implicated in the diseases [4]. Medication is used at early stages of the disease to compensate for the loss of endogenous neurotransmitter production but loses its effectiveness as the disease progresses.

[1]H. Andersson, A. Medvedev and R. Cubo are with Department of Information Technology, Uppsala University, 751 05 Uppsala, Sweden helena.andersson, alexander.medvedev, ruben.cubo@it.uu.se

B. Deep Brain Stimulation

In the 1960s, it was discovered that electrical stimulation to specific areas of the brain can alleviate symptoms in neurological disorders [5]–[7]. Today, the treatment technique has grown and DBS has been used in more than 150.000 patients worldwide [8], [9]. DBS is an approved (by FDA) treatment for a variety of conditions such as PD, ET, dystonia and obsessive-compulsive disorder [10], [11].

The DBS system is built of three parts: the electrodes, a stimulator, and a wire that connects the two [12]–[14]. The electrodes are surgically implanted deep in the brain to stimulate a certain disease-specific target. In PD patients, the electrodes are typically placed in the subthalamic nucleus (STN) or the internal segment of globus pallidus (GPi) [15]. Ventral intermediate nucleus of thalamus (VIM) or zona incerta (ZI) are used as stimulation targets in ET patients. The stimulator is implanted under the skin close to the collar bone and can be used to turn the stimulator on and off as well as change the stimulation parameters. Therefore, DBS is a reversible and flexible treatment alternative, opposed to surgical treatments of neurological disorders.

The therapeutic effect of DBS is dependent on the shape and amplitude of the stimulation impulses that are selected individually. The process of stimuli tuning is known as DBS programming and is performed manually through a time consuming trial-and-error unintuitive procedure. For instance, in PD, with regard to STN as the DBS target, one wants to stimulate the area of motor STN associated with motor symptoms but not the limbic STN, as depicted in Fig. 1. Thus accurate shaping of the electrical field is crucial.

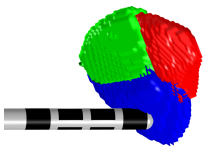

Fig. 1. Example of electrode stimulating STN. Blue: Target area of STN, associated with motor symptoms, Red: Area of STN we do not want to stimulate, associated with limbic symptoms, Green: Area of STN associated with associative symptoms.

In recent years, mathematical models of DBS have been developed to facilitate the programming and optimize the therapeutical effect. Yet, the lack of understanding of how DBS exerts its effect on targeted neural networks presents a major obstacle in connecting the electrical stimuli to the patient response.

C. The mechanism behind DBS

Dominating hypotheses that explicate the probable mechanism of DBS [16], [17] are described in more detail below.

Initially, it has been believed that DBS inhibits local neuronal elements since the treatment has similar therapeutic effects as lesion therapy. Studies have found that firings from neighbouring neurons are inhibited when DBS is targeting STN and the internal segment of the GPi [18]. STN-DBS in PD patients suppressed the neuron activity close to the place of stimulation, with a limited number of neurons being completely inhibited [19]. These effects could also be seen in GPi-DBS, but with a more prevalent part of the neurons completely inhibited [20]. The inhibition theory can as a result be underpinned by three possible mechanisms: depolarization block, inactivation of voltage-gated current, and activation of inhibitory afferents [19]–[24].

Excitation theory, on the contrary, hypothesizes that the DBS treatment excites local neural elements. GPi neurons were directly excited by GPi-DBS, but thalamic neurons were somewhat inhibited through the inhibitory GPi-thalamic projections [24], [25]. STN-DBS on the other hand increased firings in GPi, GPe and SNr neurons through excitatory projections [26], [27].

McIntyre *et al.* [16] and Kringelbach *et al.* [28] argue that the firing within the cell body and the axon are exclusive events. Suprathreshold stimulation will generate inhibition of firing in the soma, whilst also activating the axon. Direct activation of the thalamocortical relay neurons causes inhibition of intrinsic firing of presynaptic terminals under the threshold required for activation. This concept supports the idea of excitation within the pathological network as the therapeutic mechanism behind DBS.

Vreeswijk *et al.* [29] found that inhibition (inhibitory synaptic coupling) synchronized neural firing, under the condition that the duration of the action potential was shorter than the rise time of the synaptic response. On the other hand, if the rise time of the synapse is short or the action potential is broad, excitation synchronizes firing. Excitation during an action potential will lead to a delay in the next spike and excitation during the interval between spikes will advance it.

Chiken *et al.* [17] suggest a disruption theory where the abnormal information flow is disrupted by DBS. Abnormal firing patterns, abnormally increased firing, or abnormal dynamic activity will lead to motor symptoms. Motor symptoms of PD are believed to be related to the excessive synchronized oscillatory activity in the beta frequency band (around 20Hz) in the basal ganglia. By resetting the abnormal oscillation, the symptoms can be reduced or prevented.

Several other studies discuss similar interpretations of the DBS therapy, i.e. the high-frequency stimulation (HFS) suppressing the abnormal activity and instead generating a new activation pattern in the network for PD patients [18], [19], [23], [30], [31]. Furthermore, McConnell *et al.* [32] suggests that regular temporal pattern HFS STN-DBS is more effective in suppressing the low frequency oscillations in hemiparkinsonian rats.

Nevado-Holgado *et al.* [33] developed a mathematical model of the basal ganglia to gain further understanding about the beta neuronal oscillations and how and where in the brain they are generated. Pasillas-Lépine *et al.* [34] depeloped a closed-loop strategy for DBS. They discuss that restoring the stability of the firing-rate dynamics might have positive effects on Parkinsonian symptoms, due to the motor symptoms being related to the beta oscillations. García *et al.* [35] hypothesize that during HFS, antidromic activation partially blocks axonal pathways.

Summarizing the current understanding of the DBS effect on neural circuits, it is important that the electrode is properly placed with respect to the stimulation target; stimulation outside of the target invokes undesirable side effects; periodical stimulation works better than asynchronous or random one; the clinically effective values of the DBS pulse characteristics are highly individual and difficult to infer from animal experiments due to anatomical differences.

This paper addresses the impact of DBS from a functional point of view. It is postulated that the modeled neuron is supposed to process input received through a dendrite from another cell and respond by firing. Due to depletion of neurotransmitters, the firing threshold of the neuron is elevated which deficiency results in neuron deactivation. Under DBS, the neuron is still able to fire due to the cumulative action of the pulsatile electrical field produced by the lead, i.e. it recovers its function. Yet, since the conditions of firing depend on the timing and the amplitude of the DBS pulse sequence, the recovery in a neural population is only partial as the neural circuitry is spatially distributed and non-uniformly oriented with respect to the lead.

The main contributions of this paper are as follows. Both inhibition and excitation of the simulated neuron due to DBS are shown to be possible, depending on the phase difference between the neural input and the DBS pulse. Since the DBS pulse sequence is periodic and not synchronized with the neural input, the effect of DBS on neural firing with moderate pulse amplitudes cannot be predicted in general. Under DBS, some impacted neurons within the stimulation target fire due to a cumulative effect of the DBS and the neural input, thus partially restoring the circuit function. For some less frequent phase shifts, the DBS pulse inhibits an impending firing and thus can suppress neuron synchronization. Therefore, the simulation results implicitly support the disruption hypothesis by Chiken *et al.* [17].

The rest of the paper is organized as follows. First, the mathematical neuron model used in the study is summarized. A general explanation of neural activation and how an action potential is generated is provided. The original Hodgkin–Huxley model is outlined, followed by a modified version enabling the simulation of DBS. Finally, the simulation results are presented, followed by Discussion and Conclusion.

II. Mathematical modeling of the neuron

A. Neural activation

Neural signaling consists of the generation and propagation of electrical signals [36]. The information is electrically

transmitted inside the neuron by ions [37], [38]. The ion concentration is regulated by membrane proteins called ion channels and ion pumps. The ion channels can either be gated, which means they open when stimulated, or leak channels, which are open constantly. When there is a change in membrane potential, the ion channels activate thus enabling ions to flow through the membrane.

Neuron activation/firing, occurs when the membrane potential exceeds threshold. This causes an action potential. The action potential consists of five phases: the resting phase, the threshold, depolarization, repolarization, and hyperpolarization [38], [39], as seen in Fig. 2. When a stimulus is great enough to depolarize the cell above threshold, sodium ion (Na^+) channels open allowing flow inside the neuron and resulting in an action potential. At a certain value, potassium ion (K^+) channels will open allowing flow out of the cell and inactivating the previously open Na^+ channels repolarizing the cell. The K^+ efflux will result in a change in membrane potential towards resting phase. Hyperpolarization prevents the neuron from receiving another stimuli and assures that the signal only propagates in one direction.

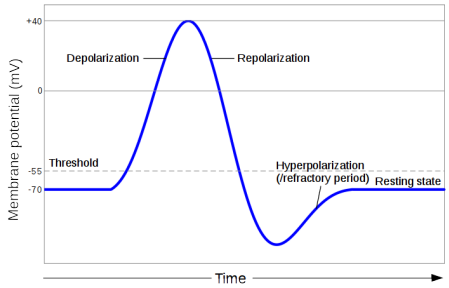

Fig. 2. Different phases of an action potential.

B. Single compartment HH model

In the 1950's Hodgkin and Huxley (HH) developed a conductance-based single-compartment model of the neuron [39]–[41]. The dynamics are captured by ionic currents that pass through the membrane and describe how an action potential is produced.

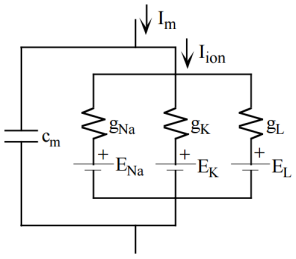

Fig. 3. Basic components of a HH electric current model representing the characteristics of the cell membrane.

The HH model is depicted in Fig. 3 as an electrical circuit representing the membrane of the neuron. The electric conductances g_{Na} and g_K portray the voltage-gated ion channels for sodium and potassium. The leak channel conductance is denoted g_l, while the capacitance over the membrane is given by C_m. The voltage sources, E_{Na}, E_K and E_l, stand for the equilibrium potentials.

The single-compartment HH model can be written as

$$\begin{aligned} I_m =& C_m \frac{dV_m}{dt} + \\ & g_K(V_m - V_K) + g_{Na}(V_m - V_{Na}) + g_l(V_m - V_l), \end{aligned} \tag{1}$$

where V_m is the membrane potential and I_m the current passing through the membrane. The parameters V_K, V_{Na}, V_l are reversal potentials. Three types of ion channels are present in (1): Na^+ channel, K^+ channel, and leak channel.

Since g_K, g_{Na}, g_l are time-dependent voltages, (1) can be rewritten as a system of four nonlinear differential equations

$$\begin{aligned} I_m =& C_m \frac{dV_m}{dt} + \\ & \bar{g}_K n^4 (V_m - V_K) + \bar{g}_{Na} m^3 h (V_m - V_{Na}) + \bar{g}_l (V_m - V_l), \\ \frac{dn}{dt} =& \alpha_n(V_m)(1-n) - \beta_n(V_m) n, \\ \frac{dm}{dt} =& \alpha_m(V_m)(1-m) - \beta_m(V_m) m, \\ \frac{dh}{dt} =& \alpha_h(V_m)(1-h) - \beta_h(V_m) h. \end{aligned} \tag{2}$$

In (2), $\bar{g}_K, \bar{g}_{Na}, \bar{g}_l$ are the maximum values of the conductances and α_n, α_m, α_h, β_n, β_m, β_h are the voltage-dependent rate constants. Further, n, m and h are gating variables, where n represents the K^+ channel activation, m and h are the Na^+ channel activation and inactivation. The gating variables are dimensionless quantities between 0 and 1. The rate constants are calculated as follows:

$$\begin{aligned} \alpha_n(V_m) =& \frac{0.01(10 - V_m)}{\exp(\frac{10 - V_m}{10}) - 1}, \quad \beta_n(V_m) = 0.125 \exp(\frac{-V_m}{80}), \\ \alpha_m(V_m) =& \frac{0.1(25 - V_m)}{\exp(\frac{25 - V_m}{10}) - 1}, \quad \beta_m(V_m) = 4 \exp(\frac{-V_m}{18}), \\ \alpha_h(V_m) =& 0.07 \exp(\frac{-V_m}{20}), \quad \beta_h(V_m) = \frac{1}{\exp(\frac{30 - V_m}{10}) + 1}. \end{aligned} \tag{3}$$

C. Multicompartmental HH model

The single-compartment HH model in (2) assumes the neuron to have the same membrane potential everywhere. To obtain a more accurate model and to understand the electrical behavior of the neuron under exogenous stimulation, a cable model where the neuron is divided into n compartments is introduced [42], [43]. Time-varying homogeneous/inhomogeneous potentials, such as an external potential surrounding the neuron and an injected current from a neighbouring neuron, have to be represented in the model. These, put together with the cable model, are illustrated in Fig. 4, where I_{inj} is the injected current, I_{axial} the axial current, and I_m the membrane current. Due to the electrical field produced by the DBS stimuli, an external potential is introduced. It is treated as a current injection in each of the n compartments and represented by I_{ext}. The multicompartmental HH model with external stimulation, results in the following equation

$$\begin{aligned} C_m^{(a)} \frac{d}{dt} V_{out,(a)}^{(a)} &= I_{inj}^{(a)} - I_m^{(a)} - I_{axial}^{(a)} - I_{ext}^{(a)}, \\ &= I_{inj}^{(a)} + (G_L^{(a)} E_L^{(a)} + \sum_T G_T^{(a)} E^{(T)}) - \\ & (G_L^{(a)} + \sum_T G_T^{(a)}) V_{out,(a)}^{(a)} - \\ & \sum_b G_{(b)}^{(a)} V_{(b)}^{(a)} + \sum_b G_{(b)}^{(a)} V_{out,(b)}^{out,(a)}, \end{aligned} \tag{4}$$

where the superscripts and indices a, b correspond to two consecutively connected compartments. The currents in compartment a are $I_{inj}^{(a)}$, $I_m^{(a)}$, $I_{axial}^{(a)}$, $I_{ext}^{(a)}$. The potential difference over the membrane of compartment a is $V_{out,(a)}^{(a)} = \phi(a) - \phi(o(a)) = V_m^{(a)}$. The potential difference between the inside of a and inside of b is $V_{(b)}^{(a)} = \phi(a) - \phi(b)$, $V_{out,(b)}^{out,(a)} = \phi(o(a)) - \phi(o(b))$ is the potential difference between outside of a and outside of b, $C_m^{(a)}$ is the membrane capacitance for compartment a, and $G_{(b)}^{(a)}$ is conductance between two connected compartments. Leak channel conductance and ion channel conductance are denoted $G_L^{(a)}$, $G_T^{(a)}$, where T is the type of ion channel. Reversal potential for the leak channel and different ion channels are $E_L^{(a)}$ and $E^{(T)}$.

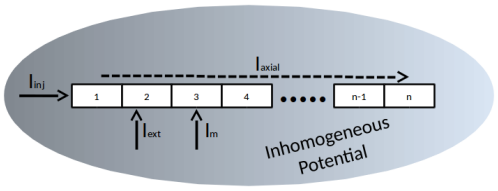

Fig. 4. Cable model with n compartments. Injected current I_{inj}, axial current I_{axial}, membrane current I_m, and external current I_{ext} are shown. I_{inj} is an injected current from a neighbouring neuron and I_{ext} comes from the inhomogeneous potential outside the neuron generated by a DBS lead.

D. Exogenous input

The cumulative impact of a single DBS pulse and injected current from another neuron on firing of the simulated one is investigated. The inputs to the neuron model are thus an external potential generated by the DBS lead and an injected current in the first compartment from a neighbouring neuron. A realistic individualized mathematical model is utilized for computing the DBS-generated potential inducing current in the axon of the simulated neuron [44].

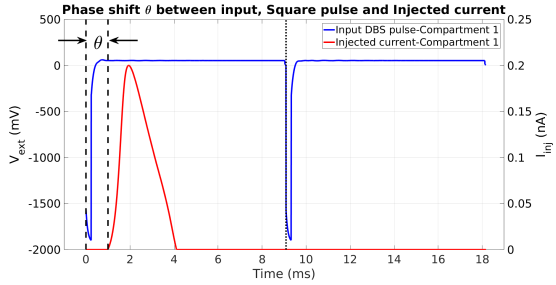

Fig. 5. Example of the input simulated neuron. DBS square pulse and injected current from a neighbouring neuron with a phase shift, θ of 1 ms. Dotted line illustrating the next DBS pulse.

Fig. 5 illustrates an example of the two inputs and the phase shift between them. Different DBS pulse widths (duty cycle) and amplitudes used in clinical practice are considered. Depending on the DBS pulse parameters and the phase shift (θ) between the two inputs, the neuron is either inhibited or excited. The minimal amplitude of the DBS pulse (A_{min}), the pulse width (PW), and the maximal amplitude of the injected current (I_{max}) will have an impact on activation of the neuron.

III. Results

The simulation results show the activation of a single neuron. It is approximated as an 1D axon with cylindrical geometry of thickness 2 μm, length 4 mm and divided into 20 sub-cylinders/compartments of equal length. The internodal length (compartment length) is approximately 100 times the thickness of the axon [1], [45], [46]. The neuron is located 0.19 mm away from the DBS lead and perpendicular to it. Fig. 6 illustrates in time domain the neuron firing under DBS without input from a neighbouring neuron.

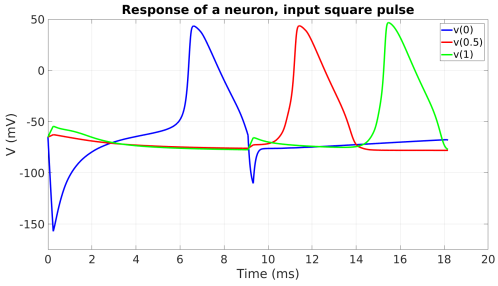

Fig. 6. Example of neuron firing under DBS, no input from neighbouring neuron. v(0) is the first compartment, v(0.5) is the middle compartment and v(1) the end compartment.

In Fig. 7 – Fig. 10, the inputs are a DBS generated square pulse and an injected current. The inputs do not activate the neuron independently, with an exception of Fig. 10(c), where the DBS input is able to activate the neuron on its own. The response to the simulation is either no activation (blue) or activation (red). Yet one can see that the DBS together with the injected current excites the neuron depending on the phase shift between the two inputs, as well as the pulse width and amplitude of the DBS pulse.

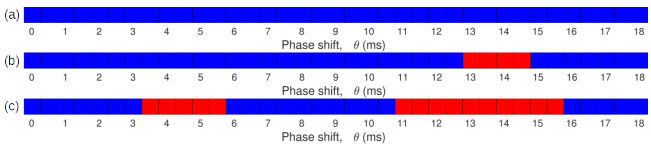

Fig. 7. Red - firing, blue - not firing. $A_{min} = -900mV$, PW= (a) 60μs, (b) 120μs, (c) 240μs. $I_{max} = 0.2nA$. θ – phase shift between the two inputs.

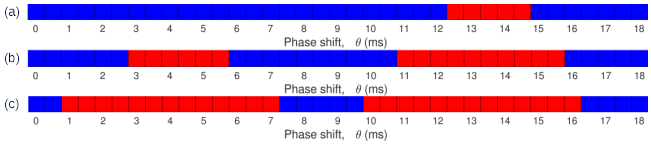

Fig. 8. Red - firing, blue - not firing. $A_{min} = -1900mV$, PW= (a) 60μs, (b) 120μs, (c) 240μs. $I_{max} = 0.2nA$. θ – phase shift between the two inputs.

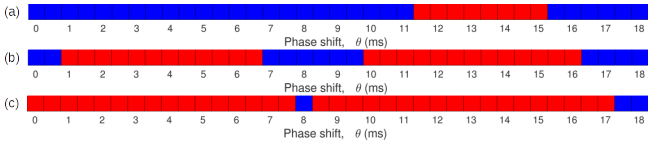

Fig. 9. Red - firing, blue - not firing. $A_{min} = -2900mV$, PW= (a) 60μs, (b) 120μs, (c) 240μs. $I_{max} = 0.2nA$. θ – phase shift between the two inputs.

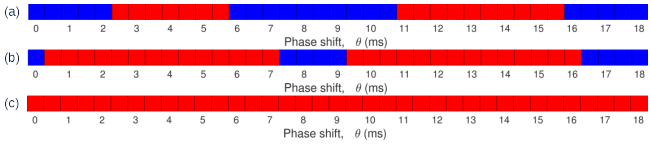

Fig. 10. Red - firing, blue - not firing. $A_{min} = -3900mV$, PW= (a) 60μs, (b) 120μs, (c) 240μs. $I_{max} = 0.2nA$. θ – phase shift between the two inputs.

The other case is when DBS suppresses an impending firing caused by an injected current. This is illustrated in Fig. 11 – Fig 14. The neuronal input activates the neuron independently and the DBS pulse does not. In Fig. 14(c) the DBS pulse is able to activate the neuron on its own. It is seen that with the added DBS input, the firing may be inhibited depending on the phase shift between the two input, as well as pulse width and amplitude of the DBS pulse.

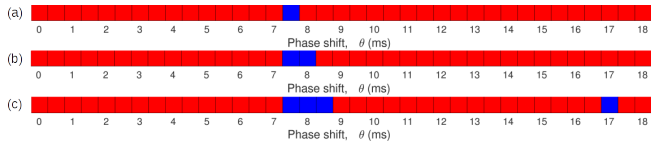

Fig. 11. Red - firing, blue - not firing. $A_{min} = -900mV$, PW= (a) 60μs, (b) 120μs, (c) 240μs. $I_{max} = 0.285nA$. θ, Phase shift between the two inputs.

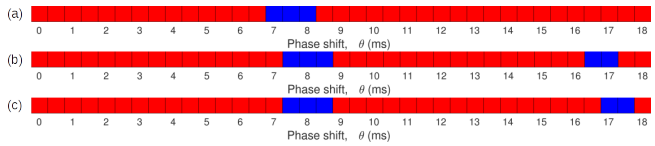

Fig. 12. Red - firing, blue - not firing. $A_{min} = -1900mV$, PW= (a) 60μs, (b) 120μs, (c) 240μs. $I_{max} = 0.285nA$. θ, Phase shift between the two inputs.

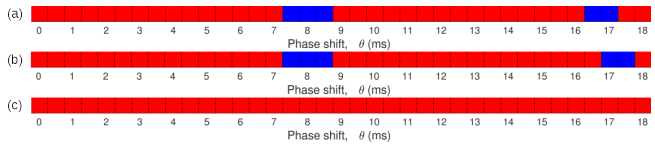

Fig. 13. Red - firing, blue - not firing. $A_{min} = -2900mV$, PW= (a) 60μs, (b) 120μs, (c) 240μs. $I_{max} = 0.285nA$. θ, Phase shift between the two inputs.

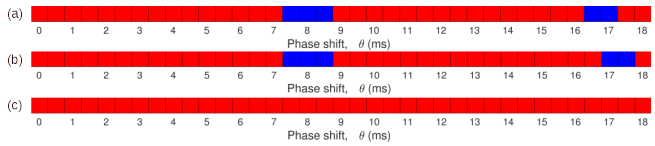

Fig. 14. Red - firing, blue - not firing. $A_{min} = -3900mV$, PW= (a) 60μs, (b) 120μs, (c) 240μs. $I_{max} = 0.285nA$. θ, Phase shift between the two inputs.

IV. Discussion

When the amplitude of the DBS pulse is large enough, the neuron fires at the same frequency as the pulse sequence. The neural output is unrelated to the input and is completely defined by the DBS. Also, when the neuronal input is large enough, firing will occur without an extra input from DBS. This corresponds to a healthy neuron. For lower input amplitudes, there is no compact interval of phase values where the DBS always activates the neuron. Firing depends on when the neuronal input occurs relative the DBS pulse. Three different situations are investigated and described below.

The first one is when neither the DBS nor the neural input activate the neuron independently. The simulation results are then depicted in Fig. 7 – Fig. 10. Here, excitation develops when the amplitude and the duty cycle of the DBS pulse are large enough to excite the neuron and for certain phase shift between the two inputs. In Fig. 7(b), Fig. 8(a), and Fig. 9(a), a buildup in membrane voltage enables the neuron to fire after the second DBS pulse. Longer pulses are more likely to produce a firing in response to injected current. This is seen in Fig. 7(c), Fig. 8(c), Fig. 9(c), Fig. 10(c) compared to Fig. 7(a), Fig. 8(a), Fig. 9(a), Fig. 10(a). Pulses of durations under 60μs lead to a focusing of the neurostimulation effect on smaller diameter axons close to the electrode while avoiding stimulation of distant pyramidal tract fibers [47]. Also, larger pulse amplitudes increase the likelihood of activation for different phase shifts.

In Inhibition, illustrated in Fig. 11 – Fig. 14, the neuronal input is able to activate the neuron independently of DBS. Although, with an added DBS pulse, the activation is suppressed for certain phase shifts between the inputs. Suppression of firing can be seen as a complete loss of processing ability in the neuron, equivalent to surgical removal. As seen in Fig. 11(a) and Fig. 12(a), for short pulses and small amplitudes, the DBS pulse is less likely to suppress firing, compared to larger DBS parameter values, seen in Fig. 11(c) and Fig. 12(c). An exception is presented in Fig. 13(c) and Fig. 14(c), where the neuronal input together with the pulse and the pulse itself are large enough to excite the neuron.

Fig. 10(c) and Fig. 14(c) depict a situation where the DBS pulse fires the neuron independently. Firing occurs regardless of the injected current for the chosen DBS parameters.

The neuronal input as well as for what input values the neuron will activate are in principle unknown. There is no information about when a particular neuron is more or less likely to receive a neuronal input. A stochastic model describing the input needs to be available in order to optimize the DBS input for a certain type of neurons.

Neuron location and orientation relative the lead need to be taken into account when evaluating firing [48]. A neuron closer to the lead is more likely to fire than one further away. The rotation of the neuron relative the lead also impact on firing. Neurons situated perpendicular to the lead are more likely to fire than those that are parallel to it.

In the present study, only one frequency of the DBS pulse has been investigated. Low frequency might mean that the neuron has more time to recover and go back to its resting condition between the DBS pulses.

V. Conclusions

A simulation study highlighting the role of the DBS in partial recovery of input processing function in the stimulated neuron is presented. It is demonstrated that a neuron that would not activate from a neuronal input alone can still fire with help of a DBS pulse. However, the effect of the stimulation greatly depends on the phase shift between the neural input and the DBS sequence. In contradiction, for certain values of the phase shift the DBS can suppress an impeding activation of the neuron. The study reveals that the intervals of phase values that assist and suppress firing are not necessarily unique within a period of the DBS sequence, which in fact stems from high nonlinearity of the neuron. Therefore, to enable the optimization of the DBS sequence for best therapeutical effect, knowledge about the neuronal input timing and amplitude is necessary, as well as information about the location and orientation of the neuron.

Acknowledgment

The authors would like to thank Stefan Engblom and Pavol Bauer, Department of Information Technology, Uppsala Uni-

versity, Sweden, for their help with the mathematical model of the neuron used in this paper.

REFERENCES

[1] A.G. Brown. Nerve Cells and Nervous Systems: An Introduction to Neuroscience. *Springer Science & Business Media*, 2012.

[2] H. Lodish, A. Berk, and SL. Zipursky et al. Molecular cell biology, 4th edition. 2000.

[3] D. Purves and G.J. Fitzpatrick et al. editors. Neuroscience, 2nd Edition. 2001.

[4] D.S. Kern and R. Kumar. Deep Brain Stimulation. *The Neurologist*, 13(5):237–252, 2007.

[5] M. Åström. Modelling, Simulation, and Visualization of Deep Brain Stimulation. *Linköping Studies in Science and Technology Dissertations*, No. 1384, 2010.

[6] J.S. Perlmutter and J.W. Mink. Deep Brain Stimulation. *The Annual Review of Neuroscience*, 29:229–257, 2006.

[7] T. Wichmann and M.R. DeLong. Deep Brain Stimulation for Neurologic and Neuropsychiatric Disorders. *Neuron*, 52:197–204, 2006.

[8] M. Hariz. My 25 Stimulating Years with DBS in Parkinson's Disease. *Journal of Parkinson's Disease*, 7:S33–S41, 2017.

[9] P. Hickey and M. Stacy. Deep Brain Stimulation: A Paradigm Shifting Approach to Treat Parkinson's Disease. *Frontiers in Neuroscience*, Vol 10, Article 173, 2016.

[10] X.L. Chen, Y.Y. Xiong, G.L. Xu, and X.F. Liu. Deep Brain Stimulation. *Intervent Neurol*, 1:200–212, 2012.

[11] A. Tekriwal and G. Baltuch. Deep Brain Stimulation: Expanding Applications. *Neurol Med Chir (Tokyo*, 55(12):861–877, 2015.

[12] R. Cubo, A. Medvedev, and H. Andersson. Deep Brain Stimulation therapies: a control-engineering perspective. *2017 American Control Conference, Seattle, WA, USA*, 2017.

[13] R. Cubo, M. Fahlström, E. Jiltsova, H. Andersson, and A. Medvedev. Semi-individualized electrical models in Deep Brain Stimulation: a variability analysis. *1st IEEE Conference on Control Technology and Applications, Hawaii, HI, USA*, 2017.

[14] T.M. Herrington, J.J. Cheng, and E.N. Eskandar. Mechanisms of deep brain stimulation. *J Neurophysiol*, 115:19–38, 2016.

[15] S. Breit, J.B. Schulz, and A.L. Benabid. Deep brain stimulation. *Cell Tissue Res*, 318:275–288, 2004.

[16] C.C. McIntyre, W.M. Grill, D.L. Sherman, and N.V. Thakor. Cellular Effects of Deep Brain Stimulation: Model-Based Analysis of Activation and Inhibition. *J Neurophysiol*, 91:1457–1469, 2004.

[17] S. Chiken and A. Nambu. Mechanism of Deep Brain Stimulation: Inhibition, Excitation, or Disruption? *The Neuroscientist*, 22(3):313–322, 2016.

[18] M. Filali, W.D. Hutchison, V.N. Palter, A.M. Lozano, and J.O. Dostrovsky. Stimulation-induced inhibition of neuronal firing in human subthalamic nucleus. *Exp Brain Res*, 156:274–281, 2004.

[19] W. Meissner, A. Leblois, D. Hansel, D. Dioulac, C.E. Gross, A. Benazzouz, and T. Boraud. Subthalamic high frequency stimulation resets subthalamic firing and reduces abnormal oscillations. *Brain*, 128:2372–2382, 2005.

[20] J.O. Dostrovsky, R. Levy, J.P. Wu, W.D. Hutchison, R.R. Tasker, and A.M. Lozano. Microstimulation-Induced Inhibition of Neuronal Firing in Human Globus Pallidus. *J Neurophysiol*, 84(1):570–574, 2000.

[21] C. Beurrier, B. Bioulac, J. Audin, and C. Hammond. High-Frequency Stimulation Produces a Transient Blockade of Voltage-Gated Currents in Subthalamic Neurons. *J Neurophysiol*, 85:1351–1356, 2001.

[22] J-M. Deniau, B. Degos, C. Bosch, and N. Maurice. Deep brain stimulation mechanisms: Beyond the concept of local functional inhibition. *European Journal of Neuroscience*, 32:1080–1091, 2010.

[23] Y. Liu, N. Postupna, J. Falkenberg, and M.E. Anderson. High frequency deep brain stimulation: What are the therapeutic mechanisms? *Neuroscience and Biobehavioral Reviews*, 32:343–351, 2008.

[24] M.D. Johnson and C.C. McIntyre. Quantifying the Neural Elements Activated and Inhibited by Globus Pallidus Deep Brain Stimulation. *J Neurophysiol*, 100:2549–2563, 2008.

[25] K.W. McCairn and R.S. Turner. Deep Brain Stimulation of the Globus Pallidus Internus in the Parkinsonian Primate: Local Entrainment and Suppression of Low-Frequency Oscillations. *J Neurophysiol*, 101:1941–1960, 2009.

[26] R. Reese, A. Leblois, F. Steigerwald, M. Pötter-Nerger, J. Herzog, H.M. Mehdorn, G. Deuschl, W.G. Meissner, and J. Volkmann. Subthalamic deep brain stimulation increases pallidal firing rate and regularity. *Experimental Neurology*, 229:517–521, 2011.

[27] S. Galati, P. Mazzone, E. Fedele, A. Pisani, A. Peppe, M. Pierantozzi, et al. Biochemical and electrophysiological changes of substantia nigra pars reticulata driven by subthalamic stimulation in patients with Parkinson's disease. *European Journal of Neuroscience*, 23:2923–2928, 2006.

[28] M.L. Kringelbach, N. Jenkinson, S.L.F. Owen, and T.Z. Aziz. Translational principles of deep brain stimulation. *Nature Reviews Neuroscience*, 8:623–635, 2007.

[29] C. Van Vreeswijk, L.F. Abbott, and G.B. Ermentrout. When Inhibition not Excitation Synchronizes Neural Firing. *Journal of Computational Neuroscience*, 1:313–321, 1994.

[30] L. Garcia, G. D'Alessandro, B. Bioulac, and C. Hammond. High-frequency stimulation in Parkinson's disease: more or less? *TRENDS in Neurosciences*, 28(4):209–216, 2005.

[31] G.C. McConnell, R.Q. So, J.D. Hilliard, P. Lopomo, and W.M. Grill. Effective Deep Brain Stimulation Suppresses Low-Frequency Network Oscillations in the Basal Ganglia by Regularizing Neural Firing Patterns. *Journal of Neuroscience*, 32(45):15657–15668, 2012.

[32] G.C. McConnell, R.Q. So, and W.M. Grill. Failure to suppress low-frequency neuronal oscillatory activity underlies the reduced effectiveness of random patterns of deeo brain stimulation. *J Neurophysiol*, 115:2791–2802, 2016.

[33] A.J. Nevado-Holgado, J.R. Terry, and R. Bogacz. Bifurcation analysis points towards the source of beta neuronal oscillations in Parkinson's disease. *50th IEEE Conference on Decision and Control and European Control Conference, Orlando, FL, USA*, pages 6492–6497, 2011.

[34] W. Pasillas-Lépine, I. Haidar, A. Chaillet, and E. Panteley. Closed-loop Deep Brain Stimulation Based on Firing-rate Regulation. *6th Annual International IEEE EMBS Conference on Neural Engineering, San Diego, California, USA*, pages 166–169, 2013.

[35] M.R. García, M. Verwoerd, B.A. Pearlmutter, P.E. Wellstead, and R.H. Middleton. Deep Brain Stimulation may reduce Tremor by Preferential Blockade of Slower Axons via Antidromic Activation. *50th IEEE Conference on Decision and Control and European Control Conference, Orlando, FL, USA*, pages 6481–6486, 2011.

[36] E.R. Kandel, J.H. Schwartz, T.M. Jessell, S.A. Siegelbaum, A.J. Hudspeth, and S. Mack. Principles of Neural Science, Fifth Edition. 2013.

[37] F. Bezanilla. Voltage-Gated Ion Channels. *IEEE Transactions on nanobioscience*, 4(1):34–48, 2005.

[38] C.S. Schwaiger. Voltage sensor activation and modulation in ion channels. *Doctoral Thesis, Stockholm, Sweden*, 2012.

[39] R. Siciliano. The Hodkin-Huxley model-its extensions, analysis and numerics. *McGill Univ., Dept. Math. and Statist., Montreal, Canada*, 2012.

[40] A.L. Hodgkin and A.F. Huxley. A quantitative description of membrane current and its application to conduction and excitation in nerve. *J. Physiol*, 117:500–544, 1952.

[41] D.K. Sharma and A.R. Garg. Dynamics of HH Model for Excitable Neuron with Added Voltage Gated Calcium Channel. *International Journal of Computer Applications (0975-8887)*, pages 19–24, 2014.

[42] F. Fröhlich and S. Jezernik. Feedback control of Hodgkin-Huxley nerve cell dynamics. *Control Engineering Practice*, 13:1195–1206, 2005.

[43] F. Rattay, P. Lutter, and H. Felix. A model of the electrically excited human cochlear neruon i. Contribution of neural substructures to the generation and propagation of spikes. *Hearing Research*, 153:43–63, 2001.

[44] P. Bauer, S. Engblom, S. Mikulovic, and A. Senek. Multiscale modeling via split-step methods in neural firing. *Math. Comput. Model. Dyn. Syst*, 2017.

[45] L.R. Squire. Encyclopedia of Neuroscince: Volume One, Volym 1. *Academic Press*, 2009.

[46] R. Perrot, P. Lonchampt, A. C. Peterson, and J. Eyer. Axonal Neurofilaments Control Multiple Fiber Properties But Do Not Influence Structure or Spacing of Nodes of Ranvier. *The Journal of Neuroscience*, 27(36):9573–9584, 2007.

[47] M.M. Reich, F. Steigerwald, and A.D. Sawalhe et al. Short pulse width widens the therapeutic window of subthalamic neurostimulation. *Ann Clin Transl Neurol*, 2(4):427–432, 2015.

[48] H. Andersson. Individualized mathematical modeling of neural activation in electric field. *Master thesis, Uppsala University*, 2017.